Chemically Derivatized n-Type Semiconducting Gallium Arsenide Photoelectrodes. Thermodynamically Uphill Oxidation of Surface-Attached Ferrocene Centers

Jeffrey M. Bolts and Mark S. Wrighton*

Contribution from the Department of Chemistry, Massachusetts Institute of Technology, Cambridge, Massachusetts 02139. *Received April 6, 1979*

Abstract: n-Type semiconducting GaAs surfaces can be derivatized using (1,1′-ferrocenediyl)dichlorosilane (I), resulting in surface-attached, electroactive, ferrocene centers. Coverage of electroactive material significantly exceeds monolayer coverage in most experiments. The surface-attached ferrocene material can be oxidized in an uphill sense by irradiating the surface with light of energy greater than 1.4 eV, the band gap of GaAs. Ferrocene can be photooxidized to 50% conversion at a potential of ~−0.25 V vs. SCE, whereas the 50% conversion occurs at a potential of +0.40 V at a reversible electrode. The ferrocene, then, can be driven uphill by greater than 0.6 V. Surface-attached, photogenerated ferricenium can in turn oxidize solution reductants such as ferrocene itself, I^-, or *N,N,N′,N′*-tetramethyl-*p*-phenylenediamine as determined by cyclic voltammetry in CH_3CN/0.1 M $[n\text{-}Bu_4N]ClO_4$ solutions. Derivatized electrodes are fairly rugged and result in modestly improved optical to electrical energy conversion compared to a naked GaAs photoelectrode-based cell employing a CH_3CN/0.1 M $[n\text{-}Bu_4N]ClO_4$ solution of ferrocene and ferricenium.

Control of interfacial charge transfer processes at semiconductor/liquid junctions is crucial to the exploitation of such interfaces in photoelectrochemical energy conversion. We have reported proof-of-concept experiments for n-type Si photoanodes which show that such electrode surfaces can be derivatized with the ferrocenes I, II, and III in order to substantially suppress the deleterious formation of insulating SiO_x on the electrode surface.[1-3] Photoanodic decomposition of n-type semiconducting electrodes is a problem common to all photoanodes,[4,5] and the technique of chemical derivatization may be generally useful in suppressing this destructive process.

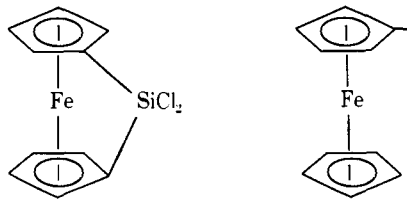

I

II

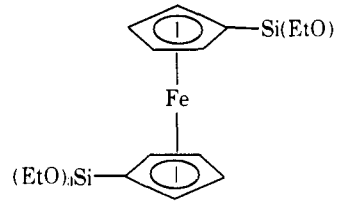

III

In this report we describe our preliminary findings concerning the chemical derivatization of pretreated, n-type GaAs surfaces using reagent I. Study of n-type GaAs is interesting, inasmuch as the material is a direct band gap, 1.4 eV, semiconductor[6] already known to yield the highest solar to electrical energy conversion efficiency (~12%)[7] for a liquid junction device. The ability to use GaAs at all hinges on the use of solution redox reagents capable of undergoing oxidation at a rate faster than anodic decomposition of the semiconductor,[8-12] and a surface treatment procedure involving the irreversible adsorption of Ru[7] gives an improvement in efficiency from ~9 to ~12%. It is also worth noting that n-type GaAs is the semiconductor used to make the highest claimed efficiency for a Schottky barrier solar cell;[13] the interface energetics for a Schottky barrier and a liquid junction cell are similar.[14]

Recently there have been two reports of GaAs surface reaction with silane reagents.[15] These results establish the viability of using electroactive reagents such as I–III, and ferrocene has been shown to be capable of efficiently capturing photogenerated holes in n-type GaAs photoanodes in nonaqueous electrolyte solutions.[16] We now describe the attachment and photoelectrochemical characterization of ferrocene reagents on n-type GaAs. Such studies establish the viability of using derivatized GaAs to effect photooxidation processes which could not be done at "naked" GaAs; in principle, anything oxidizable with ferricenium can be oxidized by photoexcitation of the derivatized GaAs.

Results

A. Photoelectrochemistry of Ferrocene at "Naked" n-Type GaAs. In order to assess the effect of derivatizing the surface of n-type GaAs with I we have examined the charge-transfer properties of ferrocene itself at "naked" (nonderivatized), n-type, single-crystal (111 face exposed) GaAs. The 111 surface of GaAs was pretreated according to the procedure outlined in the Experimental Section, and the electrolyte solution used for all studies was CH_3CN/0.1 M $[n\text{-}Bu_4N]ClO_4$. Figure 1a shows the cyclic voltammetry for ferrocene at naked n-type GaAs; the GaAs is blocking to oxidation current in the dark, but illumination of GaAs with light of energy greater than or equal to the band gap yields photoanodic current which corresponds to the ferrocene → ferricenium one-electron oxidation. The latter point is confirmed by the observation that there is no photoanodic peak in the absence of added ferrocene over the potential range shown. The current peak that is observed is diffusion limited, as stirring the solution results in an enhanced current limited by the rate of hole generation by the light. Stirring the solution also removes the cathodic return peak corresponding to the ferricenium → ferrocene reduction, since the ferricenium is swept away from the vicinity of the electrode.

The position of the photoanodic current peak is substantially more negative than at a Pt electrode. We find $E°$(ferricenium/ferrocene) to be +0.40 V vs. SCE at Pt-foil electrodes with the peak of the anodic current at ~+0.43 V vs. SCE in cyclic voltammetry. At the highest light intensity, we have observed the photoanodic peak at illuminated n-type GaAs to be at ~−0.25 V vs. SCE or ~0.68 V more negative than at Pt.

0002-7863/79/1501-6179$01.00/0

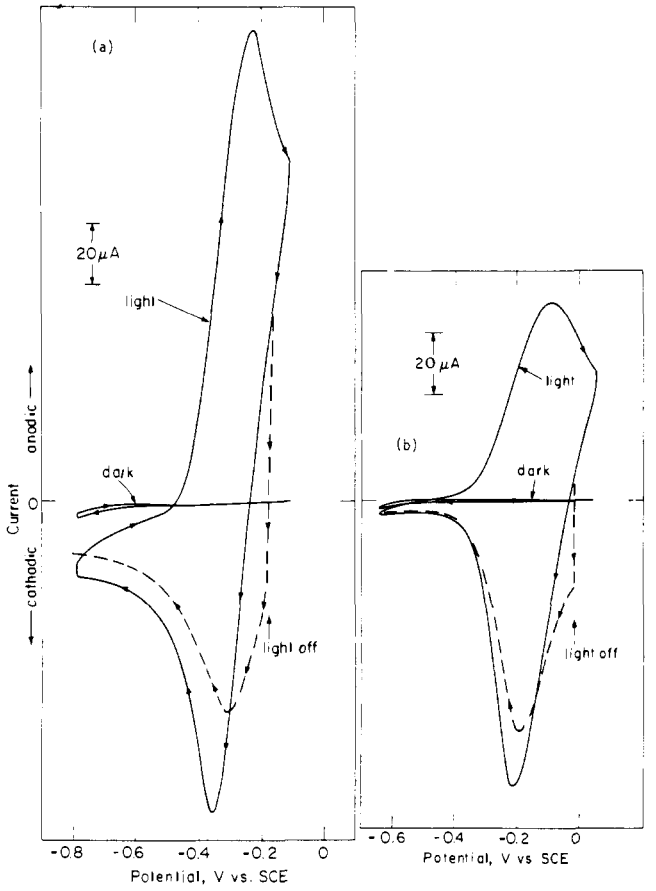

Figure 1. (a) Cyclic voltammetry of quiet $CH_3CN/0.1$ M $[n\text{-}Bu_4N]ClO_4$ solution of 5 mM ferrocene at 200 mV/s at n-type GaAs. For the illuminated case a beam expanded He-Ne, 632.8 nm, laser was used. The dashed cathodic return scan is in the dark with the illumination turned off at the indicated potential. (b) Cyclic voltammetry for n-type GaAs derivatized with I in $CH_3CN/0.1$ M $[n\text{-}Bu_4N]ClO_4$ at 100 mV/s. Illumination is from a beam expanded Ar ion laser at 514.5 nm. The dashed cathodic return scan has the same significance as in (a).

The cathodic current peak corresponding to ferricenium → ferrocene reduction appears at a more positive potential for the situation where the light is turned off at the anodic limit of the potential scan. The dark reduction does not compete with a forward photoanodic current, and accordingly the peak of the reduction current appears more positive. The prevailing rationale for observing the dark reduction peak at a potential more positive than the flat-band potential, $E_f = E_{FB}$, of the semiconductor is that surface states exist between the valence and conduction band edge positions, E_{VB} and E_{CB}, which facilitate the reduction.[12,16]

Our cyclic voltammetry studies are in essential accord with the findings previously reported,[16] though we have used a different surface treatment, GaAs orientation, and GaAs source. Our data establish the interfacial energetics to be as given in Scheme I which does not include the location of the surface states; these interfacial energetics are, within experimental error, the same as previously reported.[16]

B. Derivatization and Photoelectrochemical Characterization of n-Type GaAs. The n-type GaAs characterized by cyclic voltammetry in $CH_3CN/0.1$ M $[n\text{-}Bu_4N]ClO_4$ can be derivatized using I according to the procedure outlined in the Experimental Section. The resulting surface can be characterized by cyclic voltammetry, Figure 1b.

Cyclic voltammetry of n-type GaAs derivatized with I exhibits no anodic current in the dark, but illumination of the surface results in a photoanodic peak and a cathodic return peak of essentially equal area. The observation of these cyclic

Scheme I

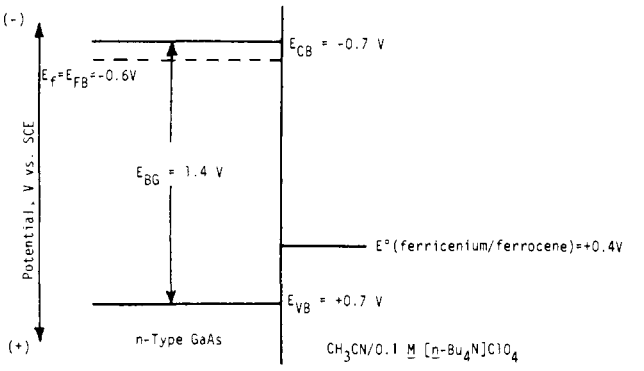

waves alone proves that the derivatization procedure results in a surface-attached, photoelectroactive reagent, since the naked GaAs over the same potential range exhibits no such waves in the absence of added ferrocene. The position of the cyclic waves for the surface-attached material is about the same as found for the solution ferrocene. This finding suggests that the surface states present on the naked surface are not substantively altered by the derivatization procedure. It is known that simply substituted ferrocenes have formal potentials close to that for ferrocene itself,[17] and attachment of I, II, or III to reversible metal electrodes such as Pt or Au gives formal potentials within 100 mV of that found for ferrocene in solution[18,19] as is generally found for attachment of reversible systems to electrode surfaces.[20] Thus, Scheme I can be taken as appropriate for n-type GaAs derivatized with I.

Figure 2 shows the light intensity dependence of the cyclic voltammetry for GaAs derivatized with I. At the lowest light intensity employed, there is no photoanodic peak. Rather, the oxidation of surface species appears to be limited by the rate of hole generation by light. As the light intensity (hole generation rate) is increased there are several noteworthy effects on the cyclic voltammetry. First, a photoanodic peak is observed. Second, the peak moves to a more negative potential and is somewhat sharper. Finally, there appears to be more integrated current for the photoanodic peak as the intensity is increased. The effects of light intensity on the electrochemistry of species confined to the surface of an n-type semiconductor have been previously discussed for n-type Si.[21] At low light intensity, the oxidation of surface material is controlled by the hole generation rate, and one observes only a small fraction of the surface material to be oxidized at the 200 mV/s scan rate where the anodic limit is only +0.2 V vs. SCE. Thus, there appears to be a limitless supply of oxidizable material. As the hole generation rate is increased by increasing the light intensity, more attached material can be oxidized over a given anodic excursion at a given scan rate, and at the highest intensities the entire amount of surface-confined material appears to be oxidized. The more negative photoanodic peak at the higher light intensity reflects oxidation in an uphill sense to a greater extent. The light-intensity dependence follows from the fact that there appears to be competing back electron transfer which is significant at low light levels but which is overcome at high hole generation rates. The ratio of surface-confined ferricenium/ferrocene is a measure of the oxidizing power of the attached material, and at a ratio of 1/1 we take the E_{redox} of the attached material to be at the formal potential, $E^\circ = +0.40$ V vs. SCE for ferricenium/ferrocene. The peak of the photoanodic current, at the highest intensity, marks the point at which the surface-confined material is ~50% oxidized; this peak occurs at an electrode potential of −0.25 V vs. SCE. For derivatized reversible electrodes (Pt or Au)[19] the peak is at ~+0.4 V, and thus illuminated, derivatized GaAs effects an uphill oxidation of ~0.6 V.

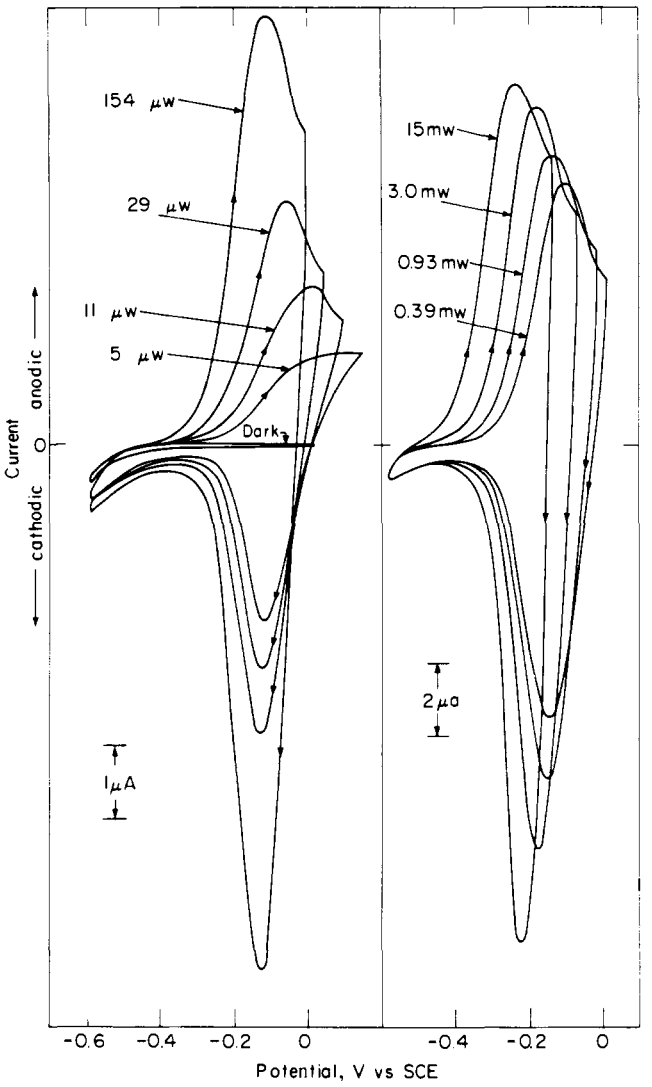

Figure 2. Light intensity (514.5 nm) dependence of the cyclic voltammetry (100 mV/s) for n-type GaAs derivatized with 1. The input optical power in μW is given at the left and in mW for the curves on the right. Note that the current scale on the left is a factor of 2 less than on the right.

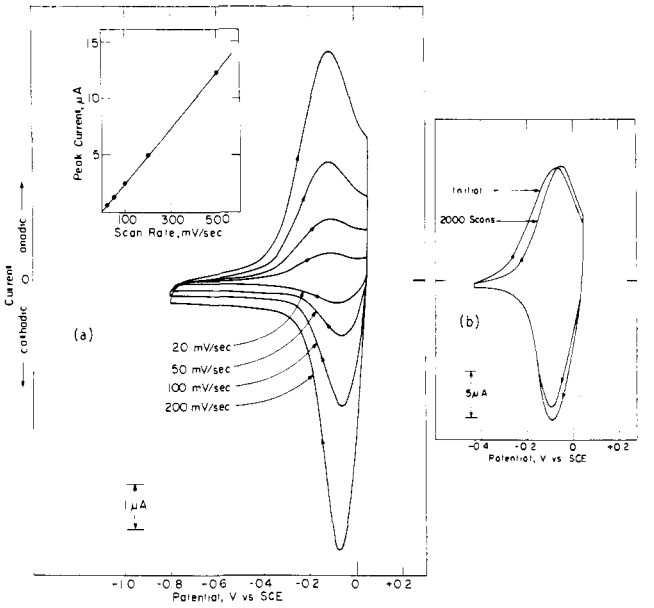

Figure 3. (a) Dependence of cyclic voltammograms on potential scan rate for n-GaAs derivatized with 1. Uniform irradiation of n-GaAs at 7.5 mW of 514.5-nm light; the electrolyte was 0.1 M $[Bu_4N]ClO_4$ in CH_3CN over a bed of activated Al_2O_3. Inset shows linear variation of peak anodic current as function of potential scan rate which is characteristic of surface-bound electroactive materials. (b) Cyclic voltammograms at 500 mV/s for n-GaAs derivatized with 1 before and after 2000 cycles between −0.44 and +0.06 V vs. SCE. Same electrode, solution, and irradiation conditions as in (a).

Integration of the cyclic voltammetric waves for derivatized n-type GaAs reveals that the coverage of redox-active ferrocene centers can exceed 10^{-9} mol/cm^2, which is substantially larger than that expected from monolayer coverage. Formation of redox-active, thick coatings on Au,[18] Pt,[18,19] Ge,[22] and Si[1-3] using 1 has been reported previously; nor is such a result unique to this system. "Dip coating" redox active polymers onto metal electrodes[23,24] or adsorbing polymeric ligands onto graphite electrodes for attachment of redox-active metal centers[25] have been reported. Treatment of GaAs surfaces with nonelectroactive silanes yields polymeric material on the surface.[15] However, even with polymeric coverages, GaAs remains the light absorber, since ferrocene has a low absorptivity.

Despite the polymeric nature of the redox-active material, the electron-transfer properties appear to be quite good. At sufficiently high light intensity, the photoanodic current peak varies little with increased scan rates and the peak current is directly proportional to scan rate up to ~500 mV/s, Figure 3. A linear scan rate dependence is expected for surface-bound reversible redox centers.[26] The width of the cyclic waves on GaAs is somewhat broader than expected for a reversible, one-electron, redox system, but we have encountered this routinely in the use of 1 to derivatize electrode surfaces.[1-3,18,19,22] We attribute the broad cyclic waves to a distribution of slightly different ferrocene centers in the polymer.

Note in Figure 3a that the cathodic current peak is at a more positive potential than is the photoanodic peak! The effect is less pronounced at the higher scan rates, since reduction is inherently sluggish at the semiconductor. This remarkable finding is not always encountered (Figures 1b, 2), but we do find this situation to be common enough that it cannot be dismissed as artifactual. This result is surprising, since the observed current for a reversible system is always a net sum of forward and reverse currents, and as such should never result in a cathodic peak which is more positive than the anodic peak unless something alters the relative importance of forward and reverse currents. For example, when we switch off the light at the anodic limit for a derivatized n-type semiconductor we have often encountered a dark cathodic current peak which is more positive than the photoanodic peak. In such cases the forward (anodic) current is simply reduced to zero by reducing the hole generation rate to zero, while the cathodic current is presumably independent of light intensity. However, in Figure 3a the data are for a continuously illuminated derivatized electrode. A rationale for the result is that when the neutral ferrocene is oxidized the attached material is cationic. The attached, positively charged material effects a change in the value of E_{FB} such that it is moved to a somewhat more positive potential. This results in a smaller barrier to cathodic current flow and changes the cathodic current potential curve such that reduction occurs at a more positive potential. Charged species absorbed onto the surface of a semiconductor are known to affect E_{FB} in such a manner.[27] In the present instance the change is modest compared to what obtains upon adsorption of S^{2-} or SH^- onto CdS.[27]

GaAs derivatized with 1 is durable. Several thousand scans back and forth between −0.4 and 0.06 V vs. SCE at 500 mV/s, resulting in the cyclical oxidation and reduction of the redox centers, can be done without substantial change in the cyclic voltammetric waves for the surface-attached ferrocene, Figure 3b. The electrodes have good "shelf life" and can be used several weeks after preparation without difficulty; derivatized

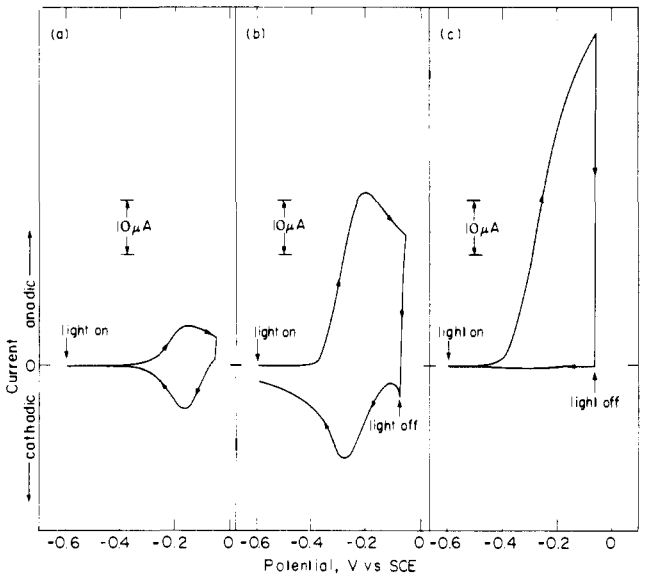

Figure 4. Cyclic voltammograms (100 mV/s) for n-type GaAs derivatized with I in (a) $CH_3CN/0.1$ M $[n\text{-}Bu_4N]ClO_4$ only, (b) in quiet electrolyte solution of 2.5 mM ferrocene, and (c) in stirred electrolyte solution of 2.5 mM ferrocene. For (b) and (c) the light was turned off at the indicated potential to measure the ferricenium reduction in the dark. Data are shown for the electrode characterized in Figure 2; here the input optical power is 0.4 mW at 514.5 nm. Voltammogram shown in (a) was unchanged after running (b) and (c).

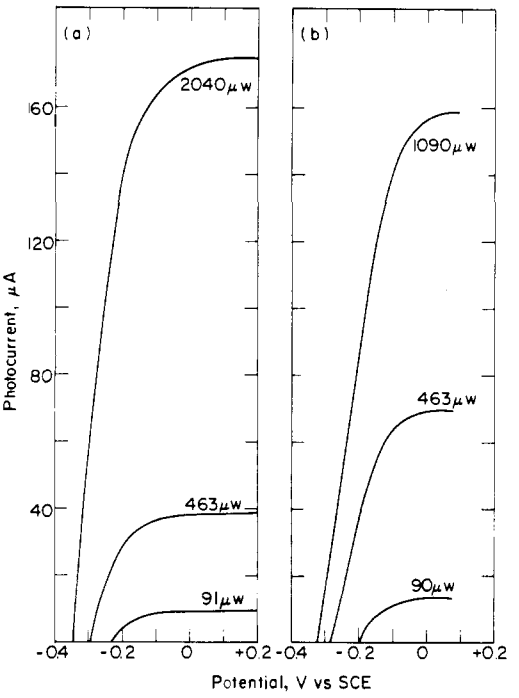

Figure 5. Equilibrium current potential scans (5 mV/s) in stirred electrolyte solution of 50 mM ferrocene, 1 mM ferricenium using the indicated input optical power in μW at 514.5 nm. To obtain photocurrent density or optical power density multiply by ~50 cm^{-2}. Curves in (a) are for naked n-type GaAs and curves in (b) are for the same crystal of GaAs but derivatized with I as characterized in Figure 1b. The derivatized electrode was unchanged before and after running curves in (b).

electrodes are generally stored at 0 °C under Ar. Anodic excursions beyond 0.2 V vs. SCE in the $CH_3CN/0.1$ M $[n\text{-}Bu_4N]ClO_4$ solution are avoided, since we observe irreversible photoanodic oxidations which result in the loss of surface-attached redox-active material.

C. Mediated Electron Transfer Using Derivatized Electrodes. As has already been pointed out for n-type Si,[1-3] a semiconductor photoanode responds to two stimuli: light and potential. This fact allows us to directly observe what we term *mediated* oxidation of a solution species. By *mediated* we mean that the photogenerated, surface-confined oxidant is responsible for oxidizing the solution reductant. In the present case, ferricenium is photogenerated on the surface of GaAs and, in principle, the photoelectrode should be useful to effect any oxidation reaction where ferricenium can be used as the oxidant. Importantly, for kinetic reasons, it may be possible to effect oxidations which are not observed at the naked GaAs. Here we illustrate how we exploit the two-stimuli response of GaAs to show that the oxidation of solution ferrocene can be photooxidized by mediated oxidation.

The key to proving that mediated oxidation obtains is that the photogenerated, surface-confined oxidant can be detected in the dark by cyclic voltammetry. Thus, cyclic voltammetry can be used to determine whether the ferricenium is reduced by the solution species. Figure 4 shows the essential results proving that ferrocene in solution can equilibrate with the ferricenium confined to the surface of the electrode. The cyclic voltammogram for the derivatized electrode in a stirred or quiet solution is the same, and turning off the light at the anodic limit allows observation of the reduction of the attached oxidant without any competing (photoanodic) forward current. Addition of ferrocene to the solution results in a larger photoanodic current peak and a larger cathodic return peak in quiet solutions; stirring the ferrocene results in an even larger photoanodic current, but the reduction peak associated with the surface-attached couple is not present. For the concentration of ferrocene used, and the scan rate employed, the photogenerated, surface-attached ferricenium is completely efficiently reduced by the solution ferrocene. Faster scan rates allow a shorter time for equilibration of the surface ferricenium and solution ferrocene, and accordingly at higher scan rates the attached ferricenium may be detected in a cathodic sweep. This is an important finding since it shows that the solution ferrocene does not simply compete with the surface ferrocene. Likewise, lower ferrocene concentrations give less reduction of surface ferricenium for a given scan rate. Proving the mediated oxidation of a solution species at a reversible electrode is difficult by the cyclic voltammetry technique, since the surface ratio of ferricenium/ferrocene will only depend on potential. If reduction of a surface ferricenium occurs on a reversible electrode, the original ratio would be reestablished, whereas dark reduction of a surface ferricenium by a solution species on GaAs is irreversible, since generation of ferricenium requires light.

Preliminary studies show that solution reductants I^- and *N,N,N′,N′*-tetramethyl-*p*-phenylenediamine (TMPD) can also be photooxidized at derivatized n-type GaAs by mediated electron transfer. Details of these studies will be given elsewhere but here we note that the ability to effect mediated electron transfer at GaAs evidences the ability to endow the surface with molecular specificity. For now we note one difficulty concerning the mediated electron transfer: it is difficult, on the basis of our present experiments, to assess just what fraction of the oxidation process is in fact mediated; that is, direct hole transfer to solution reductants is known[16] to occur and we are uncertain as to just what extent the derivatization leaves a surface having no naked areas. It is evident, though, on the basis of the ferrocene results for GaAs and for Si,[1-3] that the mediated electron transfer mechanism comprises a large fraction of the interfacial charge transfer.

D. Comparison of Naked and Derivatized n-Type GaAs. Optical to Electrical Energy Conversion. Since ferricenium/ferrocene serves as a solution couple in a photoelectrochemical conversion of light to electricity, we have compared the prop-

Table I. Output Characteristics of Naked and Derivatized n-Type GaAs[a]

photoanode	input power, μW[b]	i_{sc}, μA (Φ_e)[c]	V_{oc}, V[d]	η_{max}, % (V)[e]
naked electrode	91	9 (0.24)	0.51	3.4 (0.41)
[n-type GaAs]	463	39 (0.20)	0.58	3.2 (0.45)
	2040	175 (0.21)	0.64	3.4 (0.45)
derivatized electrode	90	13 (0.35)	0.48	4.8 (0.37)
(cf. Figure 1b)[f]	463	70 (0.36)	0.56	5.3 (0.41)
	1090	158 (0.35)	0.61	5.0 (0.39)
	1830	260 (0.34)	0.64	4.5 (0.38)

[a] In CH_3CN/0.1 M [n-Bu_4N]ClO_4 solution containing 50 mM ferrocene and 1 mM ferricenium. Illumination is at 514.5 nm; data are culled from Figure 5 except for highest intensity using derivatized electrode, which is not shown in Figure 5. [b] For input optical power density multiply by ~50 cm^{-2}. [c] i_{sc} is short-circuit current and Φ_e is the quantum efficiency for electron flow at short-circuit. For current density multiply by ~50 cm^{-2}. [d] Open-circuit photovoltage in volts. [e] Maximum efficiency for 514.5 nm → electricity; the output voltage (in volts) at the maximum power conversion efficiency is given in parentheses. [f] The derivatized electrode used for these data is characterized by cyclic voltammetry in Figure 1b.

erties of a naked and a derivatized n-type semiconducting GaAs photoanode. Equilibrium current-potential scans are shown in Figure 5. These data show that the derivatized electrode works just as well as the naked electrode, if not better. The usual comparisons to be made concern open circuit photovoltage, short-circuit photocurrent efficiency, fill factor, maximum efficiency, and voltage at the maximum power point. Table I summarizes the essential features of the data in Figure 5. We note that the open-circuit voltage and the voltage at the maximum power point are about the same in the two cases and that the rectangularity of the current-voltage curves (fill factor) is also similar. The main difference observed is that the quantum efficiency for electron flow seems to be higher for the derivatized electrode under the conditions used. This results in an overall higher efficiency for the conversion of light to electricity. Note too that there is little change in efficiency with light intensity over the range studied. These data should not be interpreted to mean that the derivatized electrode will always be substantially superior to the naked electrode in efficiency; rather, we take the data to mean that the derivatized electrode need not be substantially worse. Presumably, the derivatized electrode will be more rugged than the naked electrode owing to the protection potentially offered from surface corrosion. Experiments are underway to establish factors controlling durability and efficiency.

Summary

n-Type semiconducting GaAs can be derivatized with photoelectroactive ferrocene reagents. The redox-active material can be persistently attached and can be oxidized in an uphill sense by irradiation. We have been able to routinely prepare surfaces where the photooxidation occurs ~0.65 V more negative than at Pt, representing substantial improvement compared to our recent studies with n-type Si derivatized with the same material.[3,21] The surface-confined redox-active material does serve as an effective mediation system for the oxidation of solution species not necessarily oxidized by the naked electrode. Finally, the derivatized electrodes seem to be as efficient as the naked electrodes in transducing light to electricity in ferricenium/ferrocene-based liquid junction cells.

Experimental Section

Materials. Single-crystal Si-doped n-GaAs wafers (111 face, 0.41 mm thick) were obtained from Crystal Specialities, Inc., Monrovia, Calif. The carrier concentrations were 3.5×10^{18} cm^{-3}, and the resistivities 10^{-3} Ω cm. The wafers were sliced into squares of area ~0.2 cm^2 and mounted as electrodes as previously reported.[8] An ohmic contact between the back surface of the crystal and a coiled Cu wire lead was established with a Ga-In eutectic, and the crystal was secured with conducting Ag epoxy. The Cu wire lead was passed through a glass tube, and all exposed surfaces were covered with insulating epoxy so as to leave only the front surface of the semiconductor in contact with the electrolyte. Before use, the electrodes were etched[28,29] for 15 s in a 3:1 mixture of HNO_3-HF and rinsed with distilled water.

For derivatization, the electrodes were immersed after etching in freshly prepared 10 M KOH at 45-50 °C for 60 s and then rinsed with distilled water and with acetone. They were then exposed to solutions of ~10^{-2} M (1,1′-ferrocenediyl)dichlorosilane in Ar-purged isooctane (298 K) under Ar atmosphere for periods ranging from 4 h to overnight. The electrodes were then rinsed twice in isooctane and twice in acetonitrile, and used in photoelectrochemical cells.

Chemicals. Spectroquality acetonitrile and isooctane and reagent grade HF, HNO_3, and KOH were used as received from commercial sources. Reagent quality ferrocene was further purified by sublimation, and polarographic grade [n-Bu_4N]ClO_4 (Southwestern Analytical Chemicals) was first dried under vacuum overnight at 80 °C and then maintained in a desiccator until used. Ferricenium as the BF_4^- or PF_6^- salt was prepared according to the literature,[30] and (1,1′-ferrocenediyl)dichlorosilane was prepared as previously reported.[18]

Electrochemical Characterization. Electrochemical experiments were performed with a Princeton Applied Research Model 173 potentiostat, Model 175 voltage programmer, and Model 179 digital coulometer. The cyclic voltammograms and current-potential curves were recorded on a Houston Instrument 2000 XY recorder. The light source at 632.8 nm was a Coherent Radiation Model 80S He-Ne laser, and, at 514.5 nm, a Spectra-Physics Model 164 Ar ion laser. Light intensities were adjusted with Corning colored glass filters and monitored with a beam splitter and a Tektronix J16 digital radiometer with J6502 probe.

The experiments were performed in single-compartment Pyrex cells equipped with saturated calomel reference electrode (SCE), Pt gauze cathode (80 mesh, ~1 × 3 cm), and n-type GaAs anode. The solvent was CH_3CN, and in all cases the supporting electrolyte was 0.1 M [n-Bu_4N]ClO_4. Generally, all experiments were performed under Ar, but neither O_2 nor the moisture from air or the SCE proved to be a serious difficulty on the time scale of the experiments reported here.

Acknowledgments. We thank the U.S. Department of Energy, Office of Basic Energy Science, for support of this research. M.S.W. acknowledges support as a Dreyfus Teacher-Scholar Grant recipient, 1975-1980.

References and Notes

(1) Wrighton, M. S.; Austin, R. G.; Bocarsly, A. B.; Bolts, J. M.; Haas, O.; Legg, K. D.; Nadjo, L.; Palazzotto, M. C. *J. Am. Chem. Soc.* **1978**, *100*, 1602.
(2) Bolts, J. M.; Bocarsly, A. B.; Palazzotto, M. C.; Walton, E. G.; Lewis, N. S.; Wrighton, M. S. *J. Am. Chem. Soc.* **1979**, *101*, 1378.
(3) Wrighton, M. S.; Bolts, J. M.; Bocarsly, A. B.; Palazzotto, M. C.; Walton, E. G. *J. Vac. Sci. Technol.* **1978**, *15*, 1429.
(4) Bard, A. J.; Wrighton, M. S. *J. Electrochem. Soc.* **1977**, *124*, 1706.
(5) Gerischer, H. *J. Electroanal. Chem.* **1977**, *82*, 133.
(6) Barrie, R.; Cunnell, F. A.; Edmond, J. T.; Ross, I. M. *Physica (Utrecht)* **1954**, *20*, 1087.

(7) Parkinson, B. A.; Heller, A.; Miller, B. *Appl. Phys. Lett.* **1978**, *33*, 521.
(8) Ellis, A. B.; Bolts, J. M.; Kaiser, S. W.; Wrighton, M. S. *J. Am. Chem. Soc.* **1977**, *99*, 2848.
(9) Chang, K. C.; Heller, A.; Schwartz, B.; Menezes, S.; Miller, B. *Science* **1977**, *196*, 1097.
(10) Ellis, A. B.; Kaiser, S. W.; Bolts, J. M.; Wrighton, M. *J. Am. Chem. Soc.* **1977**, *99*, 2839.
(11) Hodes, G.; Manassen, J.; Cahen, D. *Nature (London)* **1976**, *261*, 403.
(12) (a) Kohl, P. A.; Bard, A. J. *J. Am. Chem. Soc.* **1977**, *99*, 7531. (b) Frank, S. N.; Bard, A. J. *Ibid.* **1975**, *97*, 7427.
(13) Stirn, R. J.; Yeh, Y. C. M. *Appl. Phys. Lett.* **1975**, *27*, 95.
(14) Gerischer, H. *J. Electroanal. Chem.* **1975**, *58*, 263.
(15) (a) Haller, I. *J. Am. Chem. Soc.* **1978**, *100*, 8050. (b) Brosset, D.; Ai, B.; Segui, Y. *Appl. Phys. Lett.* **1978**, *33*, 87.
(16) Kohl, P. A.; Bard, A. J. *J. Electrochem. Soc.* **1979**, *126*, 59.
(17) Janz, G. J.; Tomkins, R. P. T. "Nonaqueous Electrolytes Handbook", Vol. II; Academic Press: New York, 1973; and references cited therein.
(18) Wrighton, M. S.; Palazzotto, M. C.; Bocarsly, A. B.; Bolts, J. M.; Fischer, A. B.; Nadjo, L. *J. Am. Chem. Soc.* **1978**, *100*, 7264.
(19) Wrighton, M. S.; Austin, R. G.; Bocarsly, A. B.; Bolts, J. M.; Haas, O.; Legg, K. D.; Nadjo, L.; Palazzotto, M. C. *J. Electroanal. Chem.* **1978**, *87*, 429.
(20) Lenhard, J. R.; Rocklin, R.; Abruna, H.; Willman, K.; Kuo, K.; Nowak, R.; Murray, R. W. *J. Am. Chem. Soc.* **1978**, *100*, 5213.
(21) Bocarsly, A. B.; Walton, E. G.; Bradley, M. G.; Wrighton, M. S. *J. Electroanal. Chem.*, **1979**, *100*, 283.
(22) Bolts, J. M.; Wrighton, M. S. *J. Am. Chem. Soc.* **1978**, *100*, 5257.
(23) Merz, A.; Bard, A. J. *J. Am. Chem. Soc.* **1978**, *100*, 3222.
(24) Van de Mark, M.; Miller, L. *J. Am. Chem. Soc.* **1978**, *100*, 3223.
(25) Oyama, N.; Anson, F. C. *J. Am. Chem. Soc.* **1979**, *101*, 739.
(26) Laviron, E. *J. Electroanal. Chem.* **1972**, *39*, 1.
(27) Ginley, D. S.; Butler, M. A. *J. Electrochem. Soc.* **1978**, *125*, 1968.
(28) Gatos, H. C.; Lavine, M. C. *J. Phys. Chem. Solids* **1960**, *14*, 169.
(29) Birintseva, T. P.; Pleskov, Yu. V. *Sov. Electrochem. (Engl. Transl.)* **1965**, *1*, 236.
(30) Hendrickson, D. N.; Sohn, Y. S.; Gray, H. B. *Inorg. Chem.* **1971**, *10*, 1559.

An ab Initio Molecular Orbital Study of 2- and 4-Monosubstituted Pyridines

Janet E. Del Bene

Contribution from the Department of Chemistry, Youngstown State University, Youngstown, Ohio 44555. *Received March 15, 1979*

Abstract: Ab initio molecular orbital calculations have been performed to investigate the structural, energetic, and electronic properties of the 2- and 4-R-pyridines, with R including the isoelectronic saturated groups CH_3, NH_2, OH, and F and the unsaturated groups C_2H_3 (vinyl), CHO, and CN. The equilibrium geometry of the pyridine ring is essentially unchanged in the equilibrium structures of the 2- and 4-R-pyridines, independent of the nature of the substituent and its position. In all cases, the 2-R-pyridines are more stable than the corresponding 4-R-pyridines. Except for substitution of F in the 4 position, substitution in the 2 or 4 position of a π donating group has a stabilizing effect in pyridine relative to benzene, while substitution of the π withdrawing groups CN in the 2 or 4 position or CHO in the 4 position has a destabilizing effect relative to benzene. Analyses have also been made of substituent effects on electron distributions, n and π orbital energies, and dipole moments of the substituted pyridines.

Introduction

Recent developments in experimental methods have led to the determination of the strengths of organic bases in the gas phase.[1-3] Comparisons of the gas-phase and solution data have highlighted the important role which the solvent may play in mediating the intrinsic strength of a base toward a particular acid,[4-6] and have emphasized the need for reexamining the traditional theoretical arguments concerning base strengths. Ab initio molecular orbital calculations on free bases and on associated acid–base pairs are particularly well suited for providing some of the fundamental data required for this reexamination.

An important series of organic bases for which experimentally measured base strengths in the gas phase are now available are the monosubstituted pyridines.[6] While a few ab initio molecular orbital studies of these bases and their association with acids have been reported,[6-8] there has not yet been a systematic study of the structural, energetic, and electronic properties of these bases; therefore, such a study has been initiated in this laboratory. Pyridine has already been investigated,[9] and the present study is concerned with a set of 2- and 4-monosubstituted pyridines (2- and 4-R-pyridines) with the substituents including the isoelectronic saturated groups CH_3, NH_2, OH, and F and the unsaturated groups C_2H_3 (vinyl), CHO, and CN. This study has three specific aims: (1) to determine the equilibrium structures of the 2- and 4-R-pyridines and to analyze substituent effects on these structures, especially on the geometry of the pyridine ring; (2) to compare the relative stabilities of the 2- and 4-R-pyridines and the energetic effects of substitution in pyridine relative to benzene; (3) to investigate substituent effects on electron distributions, n and π orbital energies, and dipole moments, which are important properties that influence base strengths.

Method of Calculation

Wave functions for the singlet ground electronic states of the 2- and 4-R-pyridines have been expressed as single Slater determinants Ψ:

$$\Psi = |\psi_1(1)\bar{\psi}_1(2) \ldots \psi_n(2n-1)\bar{\psi}_n(2n)|/\sqrt{(2n)!}$$

each consisting of a set of doubly occupied molecular orbitals (MOs). The MOs ψ_i are expressed as linear combinations of atomic basis functions ϕ_μ (the LCAO approximation):

$$\psi_i = \sum_\mu c_{\mu i}\phi_\mu$$

with the expansion coefficients $c_{\mu i}$ determined variationally by solving the Roothaan equations.[10] The basis set used for the MO expansions is the minimal STO-3G basis set with standard scale factors.[11]

The 2-R-pyridines were assumed to have C_s symmetry. In these molecules, an in-plane hydrogen atom (H′) bonded to X (X is the first-row atom of the substituent bonded to C_2; see Figure 1) has been oriented so that X–H′ is s-cis to N_1–C_2. For the 4-R-pyridines, the pyridine ring was assumed to have C_{2v} symmetry, with the C_4–X bond to the substituent coincident with the C_2 symmetry axis of the ring. When R is NH_2, F, or CN, the overall molecular symmetry is C_{2v}; in all other cases,

0002-7863/79/1501-6184$01.00/0